BEHAVIOUR OF INTERLOCKING GROUTED BRICK MASONRY UNDER LOW CYCLE FATIGUE LOADING

Maqsud E Nazar

Consulting Structural Engineer
NNC Consultants Pvt. Ltd.
B-2, Jaswant Chambers,
16 Okhla, New Delhi-110025

S.N. Sinha
Professor, Civil Engineering Deptt.,
Indian Institute of Technology, Delhi,
New Delhi-110016 (India)

SUMMARY

The results of 27 interlocking grouted stabilised sand-flyash brick masonry specimens tested under low cycle fatigue loading are presented in this paper. Three cases of loading at 0^0, 45^0 and 90^0 to the bed joints were considered. The brick units and masonry system developed by Prof. S.N. Sinha was used in present investigation. Eighteen specimens of size 500 mm x 700 mm x 100 mm and nine specimens of size 500 mm x 500 mm x 100 mm were tested.

Three minimum stress levels of 0, 0.25 and 0.50 times of average failure (peak) stress were considered. The specimens were tested between specified minimum and maximum stress level and member of cycles to failure were determined. The fatigue study presented here is limited to fatigue tests, in the range of approximately 6000 load cycles. It is observed that the effect of repeated compressive loading can cause reductions in the compressive strength of brick masonry as high as 24 percent of ultimate strength, for the range of tests considered in present study.

KEY WORDS : Interlocking brick, grout, axial strain, fatigue loading, plastic strain.

INTRODUCTION

The behaviour of brick masonry under uniaxial and biaxial compressive loading for monotonic conditions has been extensively investigated by numerous researchers (Atkinson and Noland 1983, Grimm 1975, Hamid and Drysdale 1981, Reddy and Gupta 2005, Walker 1995, Worthing et al. 1992 over a long period of time. But many structures are subjected to various loads, that are repetitive, such as loads due to earthquake, wind, water waves and live load fluctuation. Masonry wall panels subjected to repeated and reversed in-plane lateral loads indicate that the reduction in strength and stiffness occur with successive cycles of loading (Abrams et. al 1985, Naraine and Sinha 1989, Milad and Sinha 2000, Senthivel and Sinha 2003, Singh and Sinha 2004, Maqsud and Sinha 2006). However, very little studies has been conducted on the behaviour of masonry under compressive repetitive loading.

Cyclic compressive tests of brick masonry prisms subjected to varying amount of sustained and alternating stress levels indicate reduction in compressive strength as large as 30 percent of the static compressive strength (Abrams et al. 1985). The reductions in strength is influenced by mortar strengths, the amplitude of the alternating stress and the number of loading cycles. The fatigue process begins with the accumulation of damage at a localised region due to alternating loads, which eventually leads to formation of cracks and their subsequent propagation. Once the cracks have initiated they may grow as a result of further cyclic deformations. The fatigue behaviour of clay bricks has been investigated by Naraine and Sinha (1989) and found that the compressive strength of masonry reduced as low as 75 percent of the ultimate strength.

A sizable amount of research has been conducted on the behaviour of concrete under repetitive fatigue loadings (Shah and Chandra 1970, Raju 1970, Joseph 1963, Nordyby 1958, Shah and Winter 1983, Fardis et al. 1983, Yang et al. 1985, Peiyin et al. 2004). The S-N curve shows the relationship between the applied fatigue stress and the fatigue life of concrete (Karsan and Jirsa 1969, Sawko and Saha 1968, Hsu 1981, Rilem Committee 1984 and ACI Special Publications 1988).

Repeated compressive loading can result from significant fluctuation in live load intensity, especially if live load is the dominant gravity load. The effect of repeated compressive loading is particularly applicable to brick masonry structures having a large live load to dead load ratio. The masonry piers of a bridge is a good example of fatigue loading on the brick masonry. Since the dead load remains always with the structure and only fluctuation of live load takes place. It is important to study the fatigue behaviour of material considering it is initially loaded with permanent loads. Hence in this study a low cycle fatigue loading is performed to, two more unloading stress level other than unloading to zero stress level.

Fatigue behaviour of interlocking grouted stabilised sand-fly ash brick masonry under repetitive compressive loading has been presented in this paper. The number of cycles to failure is determined for various maximum and minimum stress levels considered. The study is limited to fatigue tests in the range of approximately upto 6000 cycles for three cases of loading at 0^0, 45^0 and 90^0 to the bed joints.

EXPERIMENTAL PROGRAM

Test Specimen

Brick masonry specimens have been constructed from interlocking grouted stabilized sand-fly ash bricks of size 200 mm x 100 mm x 100 mm (Figure 1) developed by Prof. S.N. Sinha (2002). The square and rectangular specimens that were made of these bricks measured 500 mm x 500 mm x 100 mm and 500 mm x 700 mm x 100 mm respectively. The composition of brick units, grout and their compressive strength and standard deviation are given in Table 1, based on a test of 52 brick units and 48 mortar cubes.

Table 1 : Properties of Interlocking Bricks and Grout

Type of material	Mix proportion by weight	Water cement ratio	Mean compressive strength, (N/mm^2)	Standard deviation, (N/mm^2)
Interlocking stabilized sand-fly ash brick	0.60 Coarse sand : 0.25 Fly ash : 0.15 Cement	0.55	22.1	1.53
Grout	Cement + Non-shrink material @0.50 lb per 110 lb of cement (@225 gm per 50 kg of cement)	0.40	38.30	4.25

Test specimens were made by the method developed by Prof. S.N. Sinha for interlocking bricks in stretcher bond. Layers of bricks were dry stacked without any mortar between them. Each masonry unit has both a projection and a depression on its horizontal and vertical faces. The depression is 6 mm and projection is 3 mm. When one brick is laid beside another, then the projection on one unit fit into the depression on other, leaving a gap of 3 mm. This gap is created around four faces of bricks. Then the cement grout was poured into the joints from the top, which spread all over and provided adequate bond. It facilitated construction work considerably. Three 70 mm grout cubes (control specimens) were also made for each test specimen to determine the compressive strength of the grout. The test specimens were built on 20 mm thick aluminum plates and cured under damp conditions along with the control specimens by covering them with wet jute sacks for 28 days. All test specimens were leveled and capped with gypsum plaster before testing.

Loading Arrangement

Hydraulic servo controlled compression testing machine of 4000 kN capacity was used for testing the specimens. Test specimens were placed between the platen of machine at the bottom and load cell of 4000 kN at the top. Teflon sheets of 10 mm thickness were used on the two bearing surfaces of each test specimen to minimise the effect of platen restraint. The general loading arrangement and test set up are shown in Figure 2.

Fig. 1 : Interlocking Brick

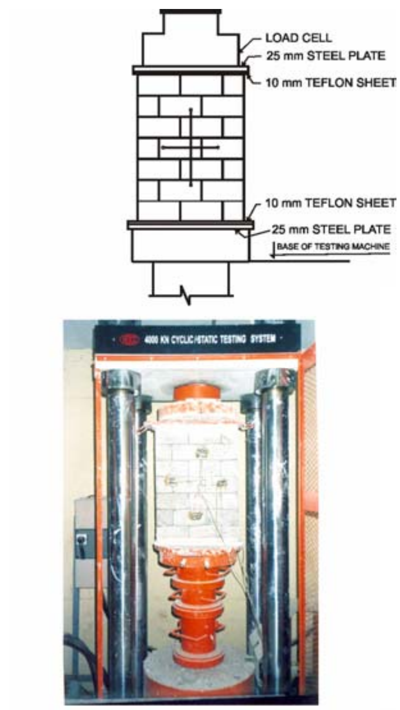

Fig. 2 : Loading Arrangement and Text Set Up

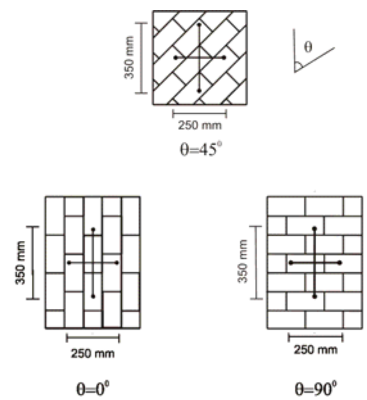

Fig. 3 : Arrangement of LVDTs and Loading Direction

Instrumentation

The interlocking grouted stabilised sand-fly ash brick masonry specimens were instrumented for the measurement of axial and lateral displacements along fixed gauge lengths, using linear variable displacement transducers (LVDTs) on both sides of specimen. The gauge lengths for axial and lateral displacements were 350 mm and 250 mm respectively. Prior trials of different positions of LVDTs and gauge lengths indicate that the position of the LVDTs as shown in Figure 3 was the most appropriate. All LVDTs and load cell were connected to data acquisition system, whereas the displacements and loads were recorded. Number of cycles were also monitored from on-line display of displacement and load on monitor for each load cycle.

Test Procedure

Tests on the interlocking grouted stabilised sand-fly ash brick masonry specimens were conducted for three cases of loading at 0^0, 45^0 and 90^0 with bed joints. Repeated axial compressive loadings between specified maximum and minimum stress levels were carried out to determine fatigue life and to examine the failure mechanism of the specimens. Each specimen was loaded in the first cycle to prescribed value of minimum and maximum stress level. The axial strains observed in first cycle of loading were ranging from $1.40\text{x}10^{-3}$ to $2.70\text{x}10^{-3}$. The applied stress corresponding to the axial strain in first cycle of loading, quantified as the maximum and minimum stress levels and were ranging from 76 to 98 percent of the average ultimate strength.

The minimum stress level was fixed at 0, 25 and 50 percent of the average ultimate strength for each case of loading. Tables 2 to 4 give the details of maximum and minimum stress levels for specimens loaded at 0^0, 45^0 and 90^0 to bed joints respectively for all the specimens tested. The maximum and minimum stress levels are normalised with average ultimate failure stress for each case of loading. From the experimental results, the average ultimate strength σ_m, for the specimens loaded at 0^0, 45^0 and 90^0 to bed joints were 12.11, 7.83 and 13.92 N/mm^2 with a standard deviation of 0.65, 0.45 and 0.28 N/mm^2 respectively. The value of axial compressive strain attained in the first cycle of loading, is normalised with respect to ε_m, the average axial strain when the peak stress is attained on the envelope stress-strain curve. The normalised axial strain attained in first cycle of loading is denoted as ε_i. From the experimental results, the average axial strain corresponding to peak stress for specimen loaded at 0^0, 45^0 and 90^0 to bed joints were $3.0x10^{-3}$, $1.72x10^{-3}$ and $2.75x10^{-3}$ with a standard deviation of $1.36x10^{-4}$, $0.54x10^{-4}$ and $1.0x10^{-4}$ respectively.

TEST RESULTS AND EVALUATION

Failure Characteristics

Failure and crack initiations of interlocking grouted stabilised sand-fly ash brick masonry specimens varied for different load cases. For specimens loaded at 0^0 to bed joints, failure occurred by splitting in vertical bed joints. The splitting initiates at free edges and gradually propagates towards the center of panel. Thereafter, the separated fragments of specimens behave like individual compression members. The failure mode were similar to the observed under monotonic loading.

In case of specimens loaded at 45^0 to bed joints, partial bond failures in joints were accompanied by splitting of bricks. For the specimens loaded at 90^0 to bed joints, cracks initiated at bed joints and later developed through the brick units. Failure in this case occurred by mechanism which usually involved a combination of unit failure and joint failure. Failure modes of specimens observed during experimental investigations are shown in Figure 4.

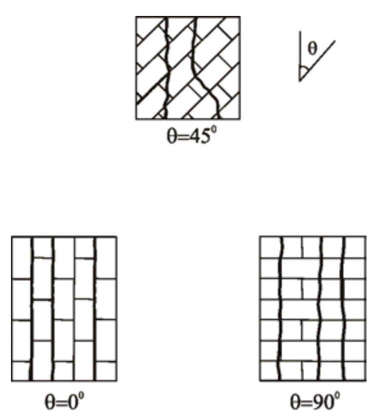

Fig. 4 : Modes of Failure

For each combination of maximum and minimum stress level considered, the number of cycles to failure, Nf, are given in Table 2 to 4 for specimen loaded at 0^0, 45^0 and 90^0 to bed

joints respectively. Failure of the interlocking grouted brick masonry specimens were characterised by the rapid increase of axial strain with increasing number of load cycles. For the range of tests considered, failure occurred at axial strain between $5x10^{-3}$ to $6x10^{-3}$ for specimens loaded at 0^0 and 90^0 to the bed joints, whereas failure occurred at axial strain between $3.0x10^{-3}$ and $3.5x10^{-3}$ for specimens loaded at 45^0 to the bed joints.

Table 2: Values of ε_i, σ_{min}, σ_{max} and Nf ($\theta=0^0$)

Specimens	ε_i	σ_{max}	σ_{min}	Nf
P1S	0.66	0.95	0.0	21
P2S	0.58	0.87	0.0	213
P3S	0.44	0.77	0.0	4910
P4S	0.70	0.96	0.25	17
P5S	0.61	0.88	0.25	224
P6S	0.48	0.79	0.25	4510
P7S	0.75	0.98	0.50	14
P8S	0.64	0.89	0.50	237
P9S	0.51	0.81	0.50	4367

Table 3: Values of ε_i, σ_{min}, σ_{max} and Nf ($\theta=45^0$)

Specimens	ε_i	σ_{max}	σ_{min}	Nf
F1S	0.78	0.96	0.0	7
F2S	0.67	0.89	0.0	72
F3S	0.59	0.76	0.0	1641
F4S	0.84	0.97	0.25	4
F5S	0.72	0.90	0.25	57
F6S	0.63	0.78	0.25	1581
F7S	0.89	0.98	0.50	3
F8S	0.77	0.92	0.50	33
F9S	0.66	0.80	0.50	1476

Table 4: Values of ε_i, σ_{min}, σ_{max} and Nf ($\theta=90^0$)

Specimens	ε_i	σ_{max}	σ_{min}	Nf
N1S	0.66	0.96	0.0	23
N2S	0.60	0.88	0.0	253
N3S	0.48	0.80	0.0	4512
N4S	0.71	0.97	0.25	19
N5S	0.63	0.90	0.25	141
N6S	0.51	0.81	0.25	6112
N7S	0.75	0.98	0.50	15
N8S	0.66	0.92	0.50	133
N9S	0.55	0.82	0.50	4947

Typical experimental fatigue stress-strain curves are shown in Figures 5 to 7 for three levels of σ_{min} considered. From these curves failure is characterised by a rapid increase of axial strain with increasing number of cycles of loading and unloading. The increase of axial compressive strains with the number of cycle is shown in Figures 8 to 16 for the three levels of σ_{min} considered. In these figures, the axial strain is normalised with respect to ε_m (i.e. axial strain corresponding to peak stress). It is denoted by ε. At high values of ε_i the increase of axial strain with the number of load cycles remained approximately linear. At lower values of $\varepsilon_{i,}$ the increase of axial strain with the number of load cycles was initially high, followed by relatively lower rate of increase of strain with the number of load cycles and finally by a rapid increase of strain near the failure.

From Tables 2 to 4, it can be observed that reduction in the strength is as high as 24 percent of the ultimate strength. Similar reduction in strength were also observed by Naraine and Sinha 1989 and Abrams et al. 1985. The tests conducted by Naraine and Sinha 1989 were on clay bricks of strength 13.1 N/mm^2 and number of load cycles were limited to 2000 cycles. Whereas, the tests conducted by Abrams et al. 1985 were done on brickwork of considerably higher strengths varying from 30.75 N/mm^2 to 18.75 N/mm^2 and load cycles were limited to 180 cycles.

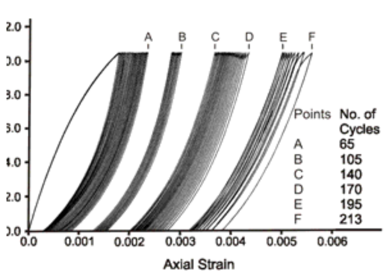

Fig. 5 : Experimental Fatigue Stress-Strain Curves ($\theta=0^0$, $\sigma_{min}=0$, $\sigma_{max}=0.87$)

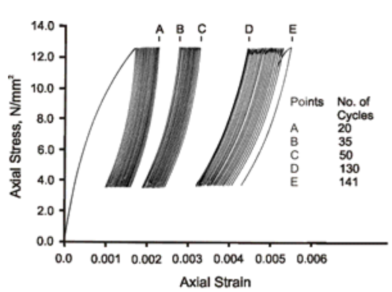

Fig. 6 : Experimental Fatigue Stress-Strain Curv ($\theta=90^0$, $\sigma_{min}=0.25$, $\sigma_{max}=0.90$)

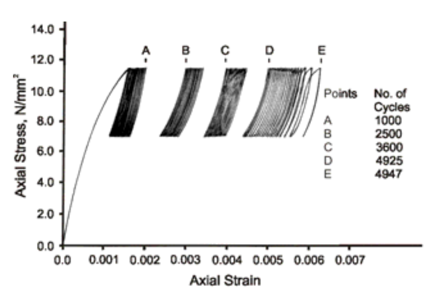

Fig. 7 : Experimental Fatigue Stress-Strain Curves ($\theta=90^0$, $\sigma_{min}=0.50$, $\sigma_{max}=0.82$)

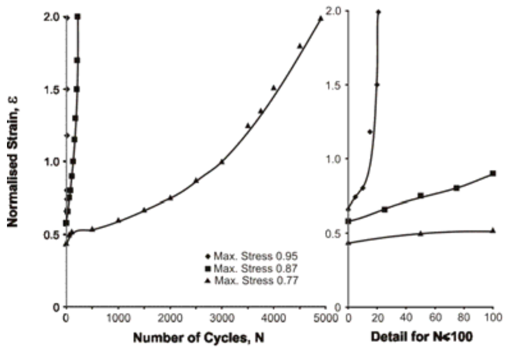

Fig. 8 : ε versus N curves (θ=0°, σ_{min}=0)

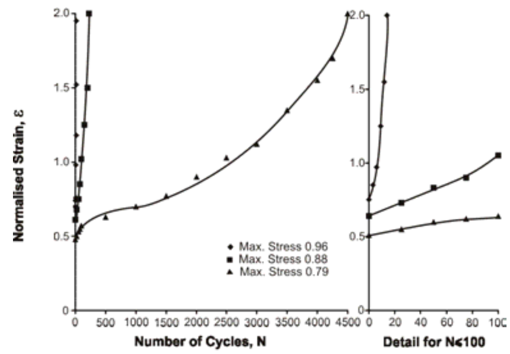

Fig. 9 : ε versus N curves (θ=0°, σ_{min}=0.25)

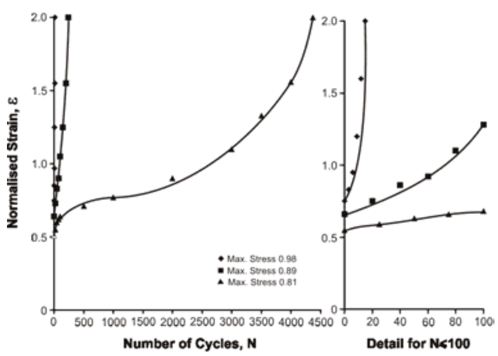

Fig. 10 : ε versus N curves (θ=0°, σ_{min}=0.50)

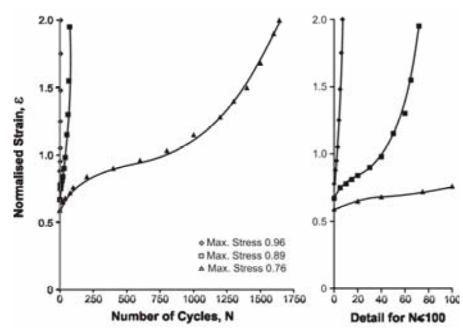

Fig. 11 : ε versus N curves (θ=45°, σ_{min}=0)

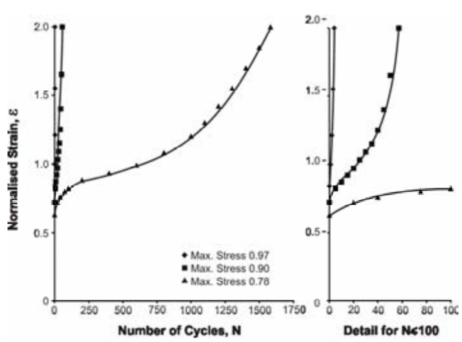

Fig. 12 : ε versus N curves (θ=45°, σ_{min}=0.25)

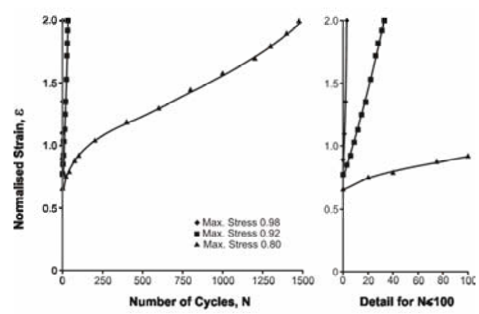

Fig. 13 : ε versus N curves (θ=45°, σ_{min}=0.50)

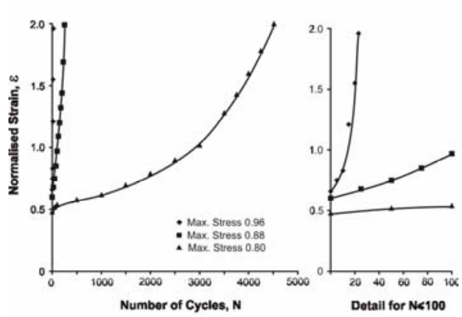

Fig. 14 : ε versus N curves (θ=90°, σ_{min}=0)

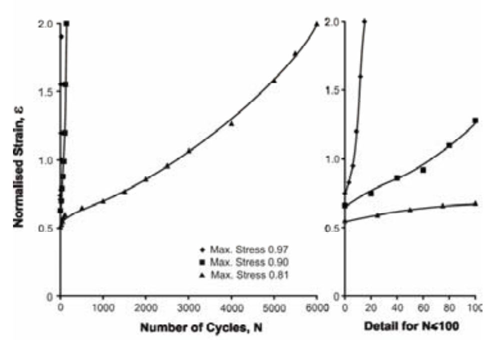

Fig. 15 : ε versus N curves (θ=90°, σ_{min}=0.25)

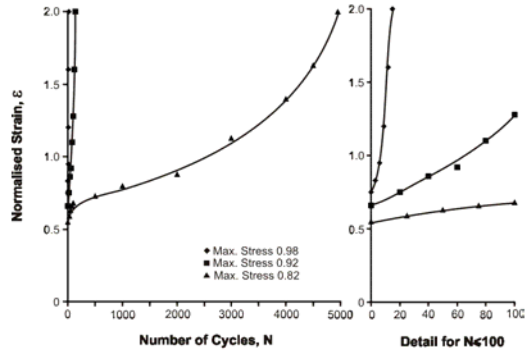

Fig. 16 : ε versus N curves (θ=90°, σ_{min}=0.50)

The data listed in Tables 2 to 4 are presented graphically in Fig. 17. The graph of ε_i versus log Nf suggest a linear variation for each level of σ_{min}, for the range of ε_i considered. It is also observed that for a given value of ε_i, the number of cycles to failure significantly increases as the value of σ_{min} increases.

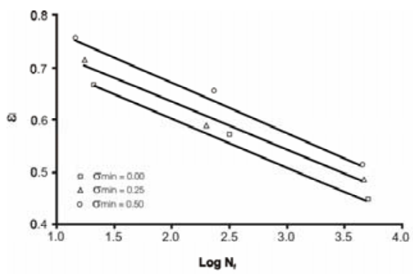

(a) θ=0°

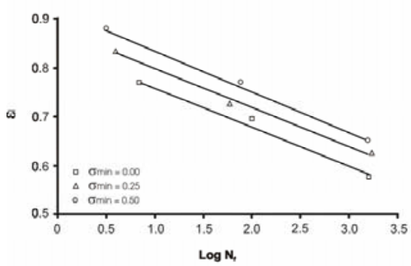

(b) θ=45°

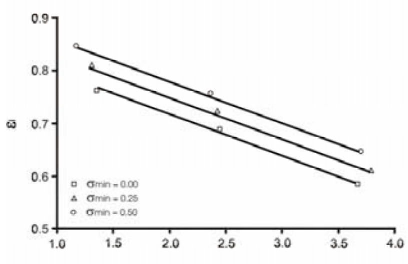

(c) θ=90°

Fig. 17 : ε_i versus Log N_f

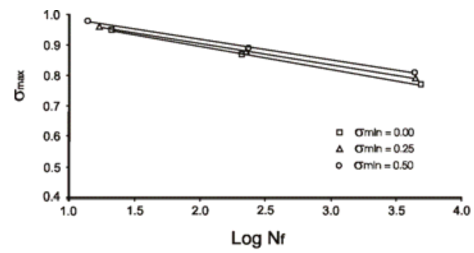

(a) θ=0°

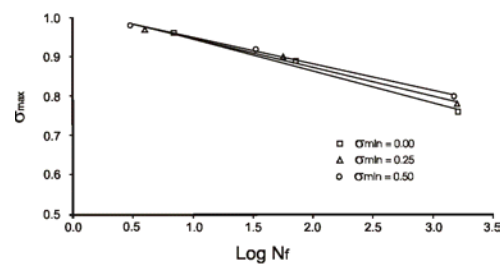

(b) θ=45°

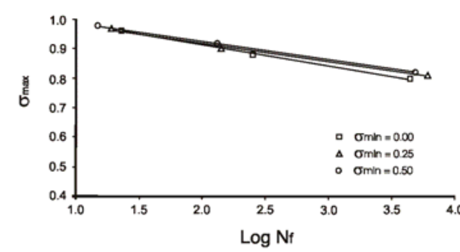

(c) θ=90°

Fig. 18 : σ_{max} versus Log N_f

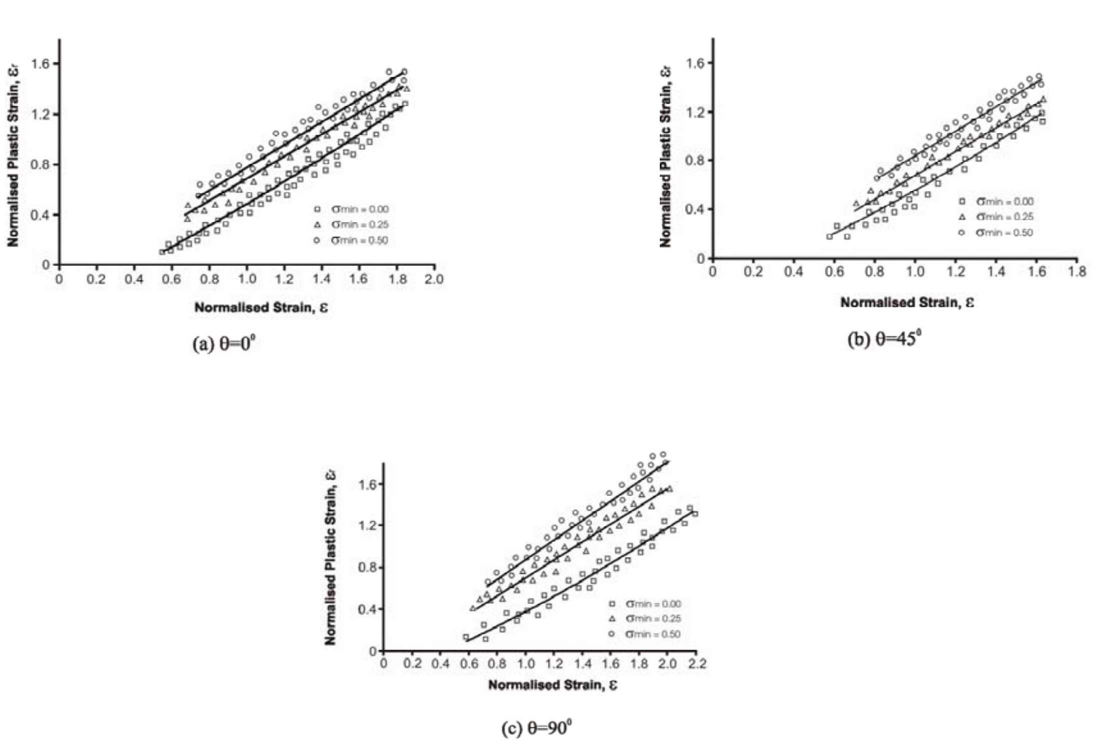

Fig. 19 : ε_r versus ε

The relationship between σ_{max} and Log Nf is presented in Figure 18 for all three cases of loading. It is observed that the number of cycles to failure increases as σ_{max} is decreases for each load case and each minimum stress level considered.

Plastic Strain

The relation between non-dimensional plastic (residual) strain, ε_r at unloading to σ_{min}, versus the non-dimensional axial strain, ε at the maximum stress level for all three cases of loading is shown in Figure 19. The strains are normalised with respect to ε_m. For σ_{min} equal to 0.25 and 0.50, the variation of ε_r with ε can be represented by a linear equation as:

$$\varepsilon_r = b\varepsilon + c \qquad (1)$$

For σ_{min} equal to zero, the variation of ε_r with ε can be represented by second order polynomial equation as:

$$\varepsilon_r = a\varepsilon^2 + b\varepsilon + c \qquad (2)$$

where

ε_r	=	Non-dimensional plastic strain
ε	=	Non-dimensional axial strain
a, b, c	=	Equation's constants whose values are given in Table 5 for all cases of loading.

Table 5 : Values of Coefficients for Plastic Strain

Bed Joint Orientation, θ	θ=0⁰				θ=45⁰				θ=90⁰			
σ_{min}	a	b	c	i_c	a	b	c	i_c	a	b	c	i_c
0	0.0709	0.7437	-0.3281	0.9554	0.1236	0.6816	-0.2492	0.9906	0.8000	0.5593	-0.2627	0.9901
0.25	-	0.8826	-0.1923	0.9885	-	0.9737	-0.2953	0.9731	-	0.8544	-0.1580	0.9942
0.50	-	0.9145	-0.1359	0.9733	-	0.9958	-0.1544	0.9539	-	0.9348	-0.0638	0.9888

The analytical curves between plastic strain and normalized axial strain are plotted in Figure 19 for each three cases of loading and degree of fit of these curves with experimental data are in the range of 0.95 to 0.99, which is a good agreement between analytical curves and test data. The values of plastic strain associated with σ_{min} equal to 0.25 and 0.50 are significantly higher than the values of plastic strain when unloading is done to zero stress level. This phenomenon may be explained by considering the shape of a typical unloading curve. A typical unloading curve initially exhibits higher stiffness at the beginning of unloading. The slope of the unloading curve gradually decreases as unloading is continued. The unloading curve considerably softness at low stress levels. Then it is being pulled inward and terminates at zero stress level.

Lateral Strain

The axial strain versus lateral strain curves obtained for the various maximum stress levels considered are shown in Figures 20 to 21 for tests conducted at each of the three levels of σ_{min}. A large variation in lateral strain at higher levels of axial strain is observed for all three cases of loading. The formation of cracks which varied in sizes and numbers in the brick masonry assemblage can be attributed to the large variation of lateral strain with axial strain.

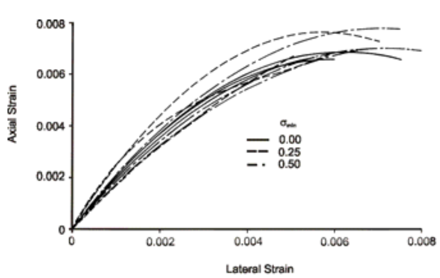

Fig. 20 : Axial Strain versus Lateral Strain Envelopes (θ=0⁰)

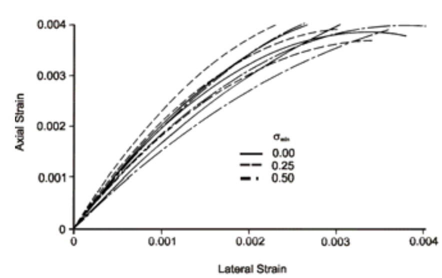

Fig. 21 : Axial Strain versus Lateral Strain Envelopes (θ=45⁰)

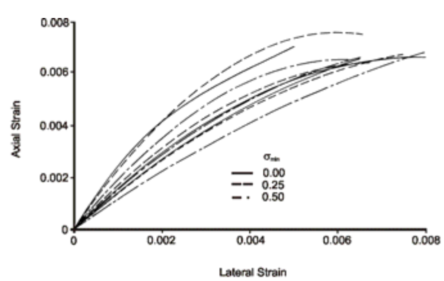

Fig. 22 : Axial Strain versus Lateral Strain Envelopes (θ=90⁰)

CONCLUSION

Based on experimental study conducted on interlocking grouted stabilized sand-fly ash brick masonry under fatigue loading, following conclusions are made:

1. The compressive strength of interlocking grouted stabilised sand-fly ash brick masonry reduced upto 24 percent under repeated compressive loading for the range of tests considered.

2. A linear relation between ε_i and Log Nf is obtained for each level of σ_{min}, for the range of ε_i considered. It is also observed that for a given value of ε_i, the number of load cycles to failure significantly increases as the value of σ_{min} increases.

3. The relationship between σ_{max} and Log N_f is also linear and showed that number of load cycles increases as the value of σ_{max} is decreases for all three cases of loading.

4. At the high value of ε_i, the increase of axial strain with the number of load cycles remained approximately linear. At lower values of ε_i, the increase of axial strain with the number of load cycles was initially high, followed by a relatively lesser rate of increase of strain with the number of load cycles and finally a rapid increase of strain near failure.

5. The plastic strain in the material with σ_{min} equal to 0.25 and 0.50 were significantly higher than the values of plastic strain when unloading was done to zero stress level.

6. A large variation in lateral strain at higher levels of axial strain was observed. This large variation can be attributed to formation of cracks which varied in numbers, sizes and locations.

REFERENCES

Abrams, D., Noland, J. and Atkinson, R., "Response of Clay Unit Masonry to Repeated Compressive Forces", Proceeding 7th International Brick Masonry Conference, Melbourne, 565-576, 1985.

Atkinson, R.H. and Noland, J.L., "A Proposed Failure Theory of Brick Masonry in Compression", Proc. 3rd Canadian Masonry Symposium, Edmonton, 5.1-5.7, 1983.

"Consideration for Design of Concrete Structures Subjected to Fatigue Loading", ACI 215R-74, Report from ACI Committee 215-Fatigue of Concrete, ACI Manual of Concrete Practice, Part 1, 25, 1988.

Fardis, M.N., Alibe, B. and Tassouas, J.L., "Monotonic and Cyclic Constitutive Law for Concrete" Journal of Engineering Mechanics, ASCE 108EM2, Proc. Paper 1781, 516-536, 1983.

"Fatigue of concrete structures", ACI-SP-75, Edited by S P, SHAH, American Concrete Institute, 1982.

Glucklich, Joseph, "Fracture of Plain Concrete" Proceedings ASCE, 89(6), 127-138, 1963.

Grimm, C.T., “Strength and Related Properties of Brick Masonry”, Journal of Structural Division, ASCE, 107(1), 217-232, 1975.

Hamid, A.A and Drysdale, R.G., “Proposed Failure Criteria for Concrete Block Masonry under Biaxial Stresses”, Journal of Structural Division, ASCE, 107(8), 1675-1687, 1981.

Karsan, I.K. and Jirsa, J.O., “Behaviour of Concrete under Compressive Loadings”, Journal of the Structural Division, ASCE, 95(12), 2543-2563, 1969.

“Long Term Random Dynamic Loading of Concrete Structures”, Report by RILEM COMMITTEE 36-RDL, Materials and Structures, 17 (97), 1984, 1-74.

Maqsud E Nazar and Sinha, S.N., “Energy Dissipation Response of Interlocking Mud Brick Masonry under Cyclic Loading”, Journal of British Masonry Society, Masonry International Vol. 19 (1), 27-40, 2006.

Milad, M.A. and Sinha, S.N., “Stress-Strain Characteristics of Brick Masonry under Uniaxial Loading”, Journal of Structural Engineering, ASCE, 125 (6), 600-604, 2000.

Naraine, K. and Sinha, S.N., “Behaviour of Brick Masonry under Cyclic Compressive Loading”, Journal of Structural Engineering, ASCE, 115 (6), 600-604, 1989.

Naraine, K. and Sinha, S.N., “Fatigue Behaviour of Brick Masonry”, STRUCENG-89, Numerical and Experimental Analysis of Structures, Los Angeles, California, 1989.

Nordyby, Gene, M., “Fatigue of Concrete–A Review of Research” ACI Journal, 55(2),191-220, 1958.

Peiyin, L.U., Qingbin, L.I. and Yupu, Song, “Damage Constitutive of Concrete under Uniaxial alternate Tension-Compression Fatigue Loading Based on Double Bounding Surfaces” International Journal of Solids and Structures, 41 (11/12),3151-3166, 2004.

Reddy, B.V.V. and Gupta, A., “Characteristics of Soil-Cement Blocks using Highly Sandy Soils”, Journal of Materials and Structures, RILEM, No. 38, 651-658, 2005.

Raju, N.K., “Comparative Study of the Fatigue Behaviour of Concrete, Mortar and Paste in Uniaxial Compression” ACI Journal, 67(6), 461-463, 1970.

Shah, S.P. and Winter, George, “Response of Concrete to repeated loading” Proceedings RILEM International Symposium on Effect of Repeated Loading of Materials and Structures, 3(23), 1967.

Shah, S.P., Chandra, S., “Fracture of concrete subjected to Cyclic Loading” ACI Journal, 67(10), 816-824, 1970.

Senthivel, R. and Sinha, S.N., “Energy Dissipation Response of Brick Masonry under Cyclic Compressive Loading”, Structural Engineering and Mechanics, 16(4), 405-422, 2003.

Singh, B.K. and Sinha, S.N., “Stress-Strain Curves for Interlocking Grouted Stabilized Mud Brick Masonry in Cyclic Uniaxial Compressive Loading”, The Third International Conference on Advances in Structural Engineering and Mechanics, Seoul, Korea, 2278-2293, 2004.

Singh, B.K. and Sinha, S.N., “Energy Dissipation in Interlocking Grouted Stabilised Mud Block Masonry under Cyclic Uniaxial Compressive Loading, 13th International Brick and Block Masonry, Conference, Amsterdam, Part-2, 1-8, 2004.

Sinha, S.N., “Masonry Building Units, Masonry System and Machine for Making Masonry Units” Indian Patent No., 676/DEL/2002.

Sawko, F and Saha, G.P., “Fatigue of Concrete and its Effect upon Prestress Concrete Beams”, Magazine of Concrete Research, 20(2), 21-30, 1968.

Hsu, T.C., ”Fatigue of Plain Concrete” Journal of American Concrete Institute, 78(4), 292-305, 1981.

Walker, P., “Strength, Durability Testing of Earth-Blocks”, Cement and Concrete Composites, 17(4), 301-310, 1995.

Worthing, G.W., Samarasinghe, W. and Lawrence, S.J. “Pressed Earth Blocks in Australia, Proc. of 4th International Seminar on Structural Masonry for Developing Countries, Madras (India), 211-216, 1992.

Yang, B.L, Dafalias, Y.F. and Herrmann, L.R., “A Bounding Surface Plasticity Model for Concrete” Journal of Engineering Mechanics, ASCE 111/EM3, Proc. Paper 19539, 359-380, 1985.